

Analysis of differentially expressed long non-coding RNAs revealed a pro-tumor role of MIR205HG in cervical cancer

LU YIN¹, YI ZHANG¹ and LEIZHEN ZHENG²

¹Department of Obstetrics and Gynecology, Changning District Maternal and Child Health Care Center, Shanghai 200050;

²Department of Oncology, Xinhua Hospital Affiliated to Shanghai Jiao Tong University School of Medicine, Shanghai 200082, P.R. China

Received November 28, 2019; Accepted June 22, 2020

DOI: 10.3892/mmr.2021.12558

Abstract. Cervical cancer is the fourth most common female malignancy for both incidence and mortality worldwide and is one of the major threats to women's health. The role of long non-coding RNAs (lncRNAs) in cervical cancer remains largely unknown. In the present study, the differentially expressed lncRNAs in cervical squamous cell carcinoma and endocervical adenocarcinoma (CESC) tissues were retrieved from The Cancer Genome Atlas (TCGA) and were analyzed. The expression analysis of related genes was performed with GEPIA. The proliferation and migratory and invasive abilities of MIR205HG knockdown CESC cells were analyzed using Cell Counting Kit-8 and transwell assays. The expression of Ki-67 and p16 was detected by immunofluorescence. A total of 203 differentially expressed lncRNAs were identified. The results demonstrated that MIR205HG was overexpressed in CESC tissues. Furthermore, the genes related to MIR205HG were enriched in cancer-related pathways. MIR205HG knockdown significantly decreased the proliferation and migratory and invasive abilities of CESC cells. In addition, silencing of MIR205HG significantly decreased the expression of p16 in C-33 A cells. The expression of fibroblast growth factor receptor 3, thymidine phosphorylase and GTPase HRas was downregulated in MIR205HG knockdown CESC cells. These findings revealed some potential lncRNA candidates for cervical cancer research and suggested that MIR205HG may have a pro-tumor role in CESC.

Introduction

Cervical cancer ranks as the fourth most common cancer diagnosed among women, with ~570,000 cases in 2018 worldwide (1). Squamous cell carcinoma and adenocarcinoma constitute the main types of cervical cancer and are associated with human papillomavirus (HPV) infection (2). Recently, increasing rates of cervical cancer in young women have been reported (3). Surgery, radiotherapy, and chemotherapy are the common therapeutic strategies for treating cervical cancer. A nine-valent HPV vaccine has been developed to prevent HPV infection (4). However, further studies are urgently needed for designing effective diagnosis and prognosis biomarkers and determining the underlying mechanisms.

Along with the mRNA coding proteins, other parts of the transcript have important roles in regulating numerous biological processes. Among these, long non-coding RNAs (lncRNAs) have been identified as a key regulators of tumor progression (5). For example, the lncRNA UCA1 is upregulated in numerous types of tumor and has been reported to promote cancer cell migration, invasion, proliferation and immune escape (6). In addition, the lncRNA *PSTAR* suppresses liver cancer cell proliferation and tumorigenesis via the p53 pathway, but does not affect apoptosis (7). The roles of various lncRNAs in cervical squamous cell carcinoma and endocervical adenocarcinoma (CESC) have been extensively studied (8). In CESC, the lncRNA (HOX transcript antisense RNA) HOTAIR is overexpressed and promotes the migration, invasion and proliferation of tumor cells (9,10). Furthermore, previous studies on biomarker-analysis have predicted six candidate lncRNAs, including TMEM220-AS1, TRAM2-AS1, C5orf66-AS1, RASSF8-AS1, AC126474 and AC004908, for cervical cancer (11). However, these lncRNAs should be validated by experimental and clinical investigation. A few studies have investigated the role of the lncRNA MIR205HG. For instance, it has been reported that MIR205HG was highly expressed in p53-mutant head and neck squamous cell carcinoma compared with p53-wild-type tumors, and promoted the proliferation of cancer cells in head and neck squamous cell carcinoma (12). MIR205HG can also inhibit the basal-luminal differentiation of human prostate basal cells by binding to the interferon regulatory factor binding site (13) and MIR205HG was reannotated as Long Epithelial Alu-interacting Differentiation-related RNA (LEDAR) (14).

Correspondence to: Dr Yi Zhang, Department of Obstetrics and Gynecology, Changning District Maternal and Child Health Care Center, 773 Wuyi Road, Changning, Shanghai 200050, P.R. China
E-mail: m13661903705@163.com

Dr Leizhen Zheng, Department of Oncology, Xinhua Hospital Affiliated to Shanghai Jiao Tong University School of Medicine, 1665 Kongjiang Road, Yangpu, Shanghai 200082, P.R. China
E-mail: LeizhenZh2019@163.com

Key words: MIR205HG, cervical cancer, long non-coding RNAs

In order to determine the potential diagnostic and therapeutic lncRNA targets in cervical cancer, the differentially expressed lncRNAs in CESC were analyzed. The role of one lncRNA in particular in regulating the proliferation and migratory and invasive abilities of CESC cell lines was subsequently investigated.

Materials and methods

Gene expression data of CESC. The transcriptome data of 306 CESC and 3 normal samples were downloaded from The Cancer Genome Atlas (TCGA) database (<https://tcga-data.nci.nih.gov/tcga/>). Among the CESC patients, 24 cases had p53 mutation and 282 cases had no p53 mutation. Furthermore, the GSE27678 dataset, which includes 14 healthy and 30 squamous cell carcinomas of cervix (including two premalignant lesions and squamous cell carcinomas cell lines), was obtained from Gene Expression Omnibus (GEO) database (<https://www.ncbi.nlm.nih.gov/geo/query/acc.cgi?acc=GSE27678>). All data were publicly available and were downloaded for research purpose.

Differentially expressed lncRNA analysis. The expression of MIR205HG was analyzed by GEPIA2 (<http://gepia2.cancer-pku.cn/#analysis>) in 306 CESC and 13 normal samples (3 normal samples from TCGA and 10 normal samples from Genotype-Tissue Expression database). The differentially expressed lncRNAs were analyzed using R software version 3.6.3 (<https://www.r-project.org/>), and a \log_2 fold change >1 was used to determine significance. GSE27678 was analyzed by GEO2R. Pathway enrichment analysis was performed using DAVID (<https://david.ncifcrf.gov/>). The top 20 enriched pathways were selected ($P < 0.05$). The bubble plots were designed using ggplot2 package of R (<http://had.co.nz/ggplot2/>). Survival and correlation analysis were performed using GEPIA2 (<http://gepia2.cancer-pku.cn/#index>). The network analysis was performed using Cytoscape V3.6.1 (<https://cytoscape.org/>).

Cell culture. Ca Ski and C-33 A cell lines were purchased from The Cell Bank of Type Culture Collection of the Chinese Academy of Sciences. Human cervical epithelial cell line (HCerEpiC) was obtained from Shanghai Zhongqiaoxin Zhou Biotechnology Co., Ltd. (cat. no. 7060). Ca Ski was cultured in RPMI 1640 (cat. no. 10-040-CV; Corning, Inc.), C-33 A was cultured in MEM (cat. no. E600020; Sangon Biotech Co., Ltd.) and HCerEpiC was cultured in DMEM (cat. no. 10-013-CV; Corning, Inc.). All media were supplemented with 10% FBS (cat. no. 10099-141-FBS; Gibco; Thermo Fisher Scientific, Inc.) and 1% penicillin-streptomycin (cat. no. E607011; Sangon Biotech Co., Ltd.). All cells were placed at 37°C in a humidified incubator containing 5% CO₂.

Reverse transcription quantitative (RT-q) PCR. Total RNA was extracted from cells using TRIzol reagent (Invitrogen; Thermo Fisher Scientific, Inc.), and reverse transcription was performed using cDNA Synthesis kit (cat. no. K1622; Thermo Fisher Scientific, Inc.) according to the manufacturers' instructions. Quantitative PCR was carried out on an ABI Q6 system (Applied Biosystems; Thermo Fisher Scientific, Inc.). RT-qPCR reactions were performed as follows: 95°C for 10 min, 45 cycles of 95°C for 15 sec, 60°C for 60 sec and a final dissociation stage.

The relative expression levels were normalized to endogenous control GAPDH and were expressed as $2^{-\Delta\Delta Cq}$ (15). The sequences of the primers used were as follows: GAPDH, forward 5'-AGA AGGCTGGGGCTCATT-3', reverse 5'-TGCTAAGCAGTT GGTGGTG-3'; MIR205HG, forward 5'-GTTTCACCATGT TGCCAGACT-3', reverse 5'-CCTGTGCGGAACAGAAAT GACT-3'; fibroblast growth factor receptor 3 (FGFR3), forward 5'-GTGCTCAAGACGGCGGGC-3', reverse 5'-GCCACGCAG AGTGATGAGAAA-3'; thymidine phosphorylase (TYMP), forward 5'-GAGTCTATTCTGGATTCAATGTCA-3', reverse 5'-AGAATGGAGGCTGTGATGAGTG-3'; and GTPase HRas (HRAS), forward 5'-CTGAGGAGCGATGACGGAAT-3' and reverse 5'-GGAATCCTCTATAGTGGGGTCGT-3'.

RNAi interference. MIR205HG-homo-474 was knocked down using small interfering (si) RNA, which was transfected into Ca Ski and C-33 A cell lines using Lipofectamine™ 2000 (Invitrogen; Thermo Fisher Scientific, Inc.). Ca Ski and C-33 A cells were seeded into a 6-well plate with 30×10^4 cells/well 1 day before transfection. Cells were transfected with MIR205HG siRNA or control siRNA with a final concentration of 50 nM, and culture for 24 h. The transfection efficiency was confirmed by RT-qPCR. The siRNA was purchased from Suzhou GenePharma Co., Ltd. The MIR205HG siRNA sequence was 5'-GCUGAACUGGGU GCUUUAUTT-3'; 5'-GCUGAACUGGGUGCUUUAUTT AUAAGCACCCAGUUCAGCTT-3', and that of the siRNA control was 5'-UUCUCCGACGUGUCACGUTT-3' and 5'-ACGUGACACGUUCGGAGAAT-3'.

Cell Counting Kit-8 (CCK-8) assay. Cell proliferation was determined using CCK-8 assay (Beyotime Institute of Biotechnology). Cells were cultured at the density of 1,000 cells/well and culture for 24 h before transfection in a 6-well plate. Each sample was assessed in six duplicates. Subsequently, 10 μ l CCK-8 was added to each well for 1 h, and absorbance was detected at 450 nm on a microplate reader (Infinite M1000; Tecan Group, Ltd.).

Transwell assay. The migratory and invasive ability of cells was analyzed using Transwell assay. The 8.0- μ m pore size membranes (cat. no. 353097; Falcon®; BD Biosciences) were used for migration assay whereas the BioCoat™ Matrigel® 0.8- μ m pore size membranes (cat. no. 354480; Corning, Inc.) were used for invasion assay. The membranes were placed in a 24-well plate, and a total of 75,000 cells were seeded in the upper chamber containing serum-free medium. A volume of 700 μ l medium containing 10% FBS was loaded into the lower chamber at the bottom of 24-well plate. The filters were stained with crystal violet (Sangon Biotech Co., Ltd.) after 24 h, at 20°C for 30 min. Cells were observed and counted under a light microscope at x200 magnification (Nikon Corporation; SMZ1000). Three random fields were counted for each microscopic field.

Immunofluorescence staining. Immunofluorescence staining was performed using the conditions suggested by the primary antibody suppliers. Briefly, coverslips were placed into the 24-well plate, and the digested cells were inoculated to the 24-well plate with a cell density of $\sim 50,000$ cells/well and 500 μ l medium, which were then cultured at 37°C for 24 h. After the cell

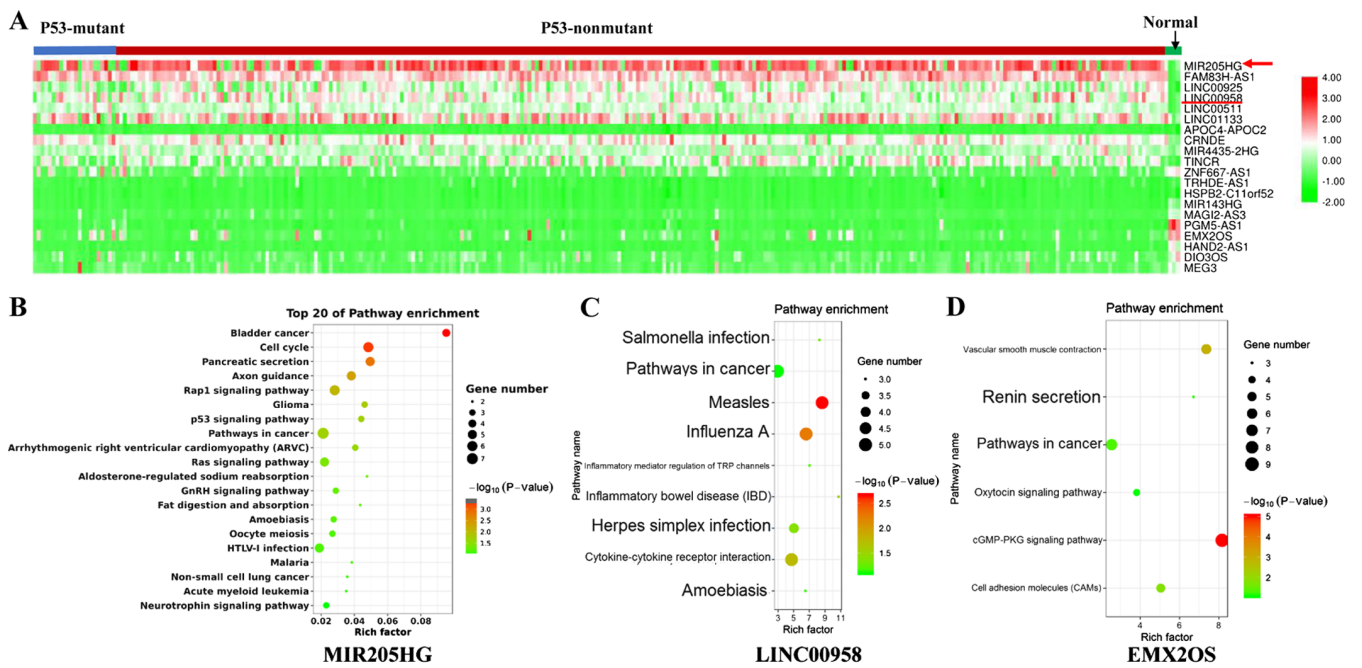


Figure 1. Analysis of lncRNA highly expressed in CESC. (A) Heatmap of the top 20 differentially expressed lncRNAs in CESC from TCGA samples (24 are P53-mutant tumors, 282 are P53-nonmutant tumors and 3 are normal samples). Rows in the heatmap correspond to the difference in expression of the lncRNAs and columns correspond to the TCGA samples. Red arrow represents the lncRNA MIR205HG. Relative expression level was colored green to red to indicate low to high, respectively. (B-D) Pathway enrichment of top 400 genes with a Pearson's correlation coefficient >0.2 for selected lncRNA (MIR205HG, LINC00958 and EMX2OS). Genes that had a fold-change >2 were analyzed using DAVID. Enriched pathways of these genes are presented. lncRNA, long noncoding RNA; CESC, cervical squamous cell carcinoma and endocervical adenocarcinoma.

fusion rate was 70%, cells were transfected with MIR205HG or control siRNA (50 nM) and cultured for 24 h. Cells were washed with PBS, fixed with 4% paraformaldehyde for 15 min at 20–25°C, and permeabilized at 20°C using 0.1% Triton X-100 and 5% BSA (cat. no. A8020; Beijing Solarbio Science & Technology Co., Ltd.) in PBS for 5–15 min. After permeation, the cells were washed with PBS three times/5 min. Cells were incubated with 200 μ l primary antibodies against Ki-67 (Cell Signaling Technology, Inc.; cat. no. 9449; 1:100; mouse mAb) and p16 (Beyotime Institute of Biotechnology; cat. no. AF1672; 1:300; rabbit mAb) at 4°C overnight. The cells were then incubated with 200 μ l Alexa Fluor® 488 labeled goat anti-mouse IgG secondary antibody (1:500; Abcam; cat. no. ab150113) and Cy3-labeled goat anti-rabbit IgG secondary antibodies (1:500; Institute of Biotechnology; cat. no. A0516) for 30 min at 20°C. The nuclei were counterstained with DAPI for 5 min. Images were obtained using fluorescence microscopy at x400 magnification (Leitz Orthoplan; Leica Microsystems GmbH).

Statistical analysis. Comparison between two groups was performed using two-tailed Student's t-test and comparison between three groups was performed by one-way ANOVA followed by Tukey's post hoc test. Statistical analyses were made using SPSS package 17.0 (SPSS, Inc.). $P < 0.05$ was considered to indicate a statistically significant difference.

Results

Differentially expressed lncRNAs in CESC tissues. Expression data of 306 CESC samples and 13 normal samples were retrieved from the TCGA. The cut-off \log_2 fold-change >1

was used. A total of 28 upregulated and 175 downregulated lncRNAs in clinical cancer types were analyzed. Using the same standard, 1,542 upregulated and 2,726 downregulated mRNAs were identified. The expression of the top 20 differentially expressed lncRNAs in each sample are presented in the heat map of Fig. 1A. The red arrow corresponds to MIR205HG, which was the most commonly upregulated lncRNA. Each column represents a sample in the CESC data retrieved from the TCGA.

Pathway enrichment analysis of the co-expression mRNA of lncRNAs. To predict the function of these lncRNAs, the top 400 coexpressed genes were selected by Spearman's correlation analysis (>0.2). Subsequently, overlaps of coexpressed and differentially expressed genes were selected. A pathway enrichment analysis was performed using DAVID. The results including MIR205HG, LINC00925 and EMX2OS are presented in Fig. 1B–D, respectively. MIR205HG-related genes were enriched in cancer-related pathways, such as ‘cell cycle’, ‘p53 signaling pathway’, ‘Ras signaling pathway’ and ‘bladder cancer’ (Fig. 1B). The LINC00958 coexpression genes were significantly enriched in pathways related to virus infection (Fig. 1C).

Overall survival rate analysis for the candidate lncRNAs. To investigate the clinical outcome of these lncRNAs, survival analysis was performed using GEPIA (Fig. 2). Nine lncRNAs, including six upregulated (Fig. 2A–F) and three downregulated (Fig. 2G–I) lncRNAs, were analyzed. Most of these lncRNAs have no significant association with overall survival (log rank $P < 0.05$). EMX2OS, which is one of the most downregulated

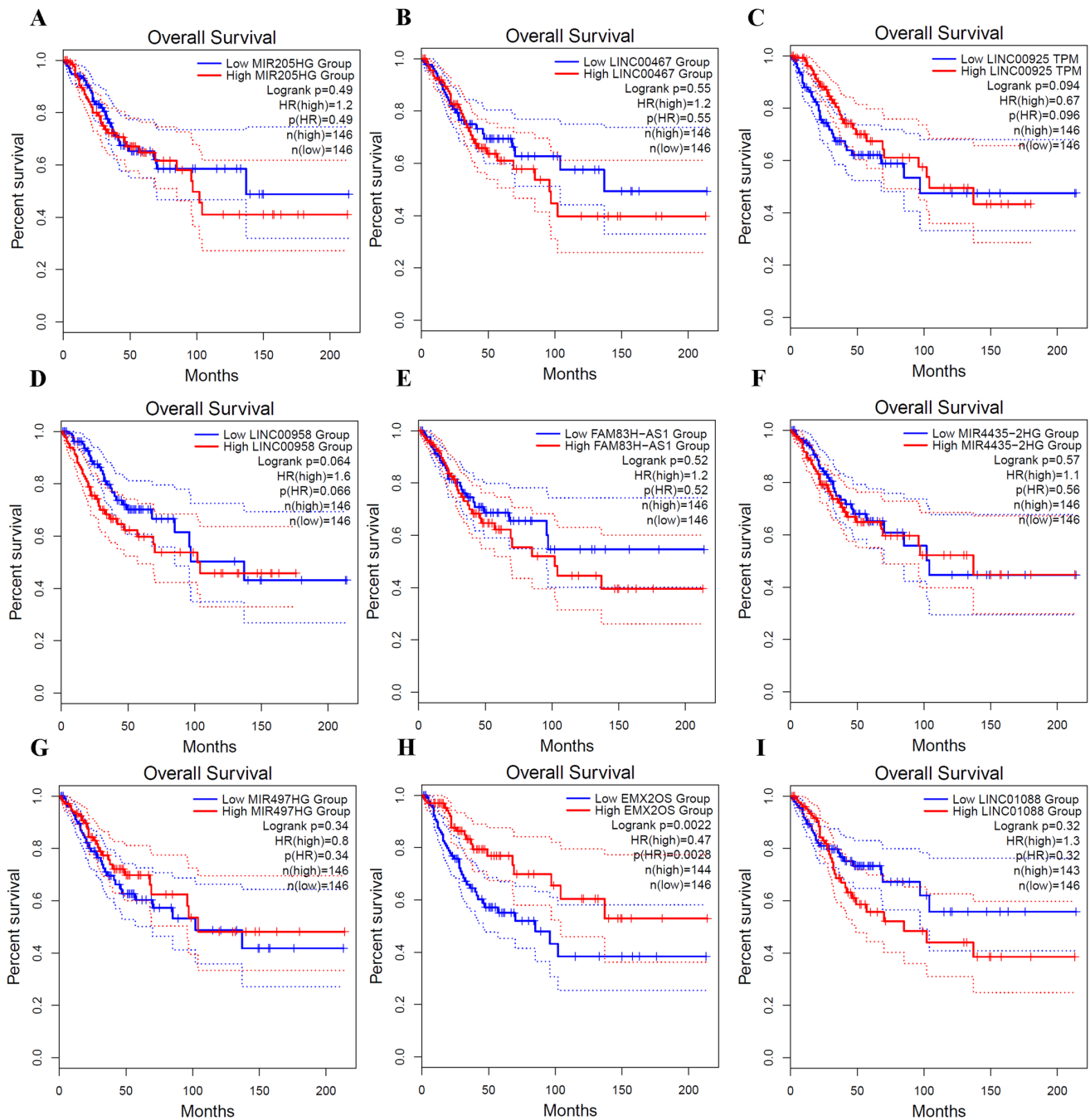


Figure 2. Overall survival rate analysis for the different expression lncRNAs. Overall survival rate for selected lncRNAs was analyzed by GEPIA. (A-F) Survival analysis results of 6 upregulated lncRNAs: (A) MIR205HG, (B) LINC00467, (C) LINC00925, (D) LINC00958, (E) FAM83H-AS1 and (F) MIR4435-2HG. (G-I) Survival analysis results of 3 downregulated lncRNAs: (G) MIR497HG, (H) EMX2OS and (I) LINC01088. lncRNA, long noncoding RNA.

lncRNAs, had a significant association with the overall survival. In addition, the EMX2OS high expression group had an improved overall survival compared with the EMX2OS low expression group (Fig. 2H). The coexpressed genes of EMX2OS were enriched in the 'cGMP-PKG signaling pathway' (Fig. 1D).

MIR205HG promotes cell migratory and invasive abilities and proliferation of CESC cells. To validate the previous results, the lncRNA MIR205HG was further studied. We analyzed the expression of MIR205HG in GSE27678 dataset, which contained 30 tumor samples and 3 normal samples. The

results demonstrated that MIR205HG had higher expression in tumors samples compared with normal samples (Fig. 3B), which was in accordance with TCGA data (Fig. 3A and B). Subsequently, the expression of MIR205HG was detected in the two CESC cell lines Ca Ski and C-33 A. The results from RT-qPCR demonstrated that MIR205HG was overexpressed in Ca Ski and C-33 A cell lines compared with the normal cervix cell line HCErEpiC (Fig. 3C). Then, MIR205HG was knockdown in Ca Ski and C-33 A cells (Fig. 4A). C-33 A and Ca Ski cell proliferation was significantly decreased following MIR205HG knockdown (Fig. 4B). Furthermore, the migratory and invasive abilities were significantly inhibited following

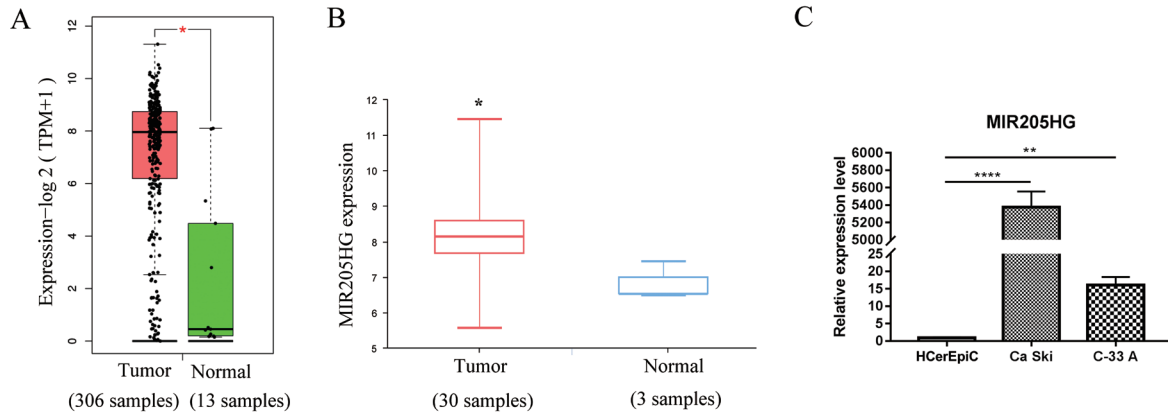


Figure 3. MIR205HG was overexpressed in CESC. (A) Expression of MIR205HG in CESC tumor samples and the normal group retrieved from GEPIA. A total of 306 tumor samples and 13 normal samples were analyzed. (B) Scatter plot representing the expression of MIR205HG from GSE27678 data. (C) Results from reverse transcription quantitative PCR indicated that MIR205HG was significantly overexpressed in the CESC cell lines Ca Ski and C-33 A compared with the normal cell line HCerEpiC. Two-tailed student's t-test. * $P < 0.05$, ** $P < 0.01$ and **** $P < 0.001$ vs. HCerEpiC group. CESC, cervical squamous cell carcinoma and endocervical adenocarcinoma.

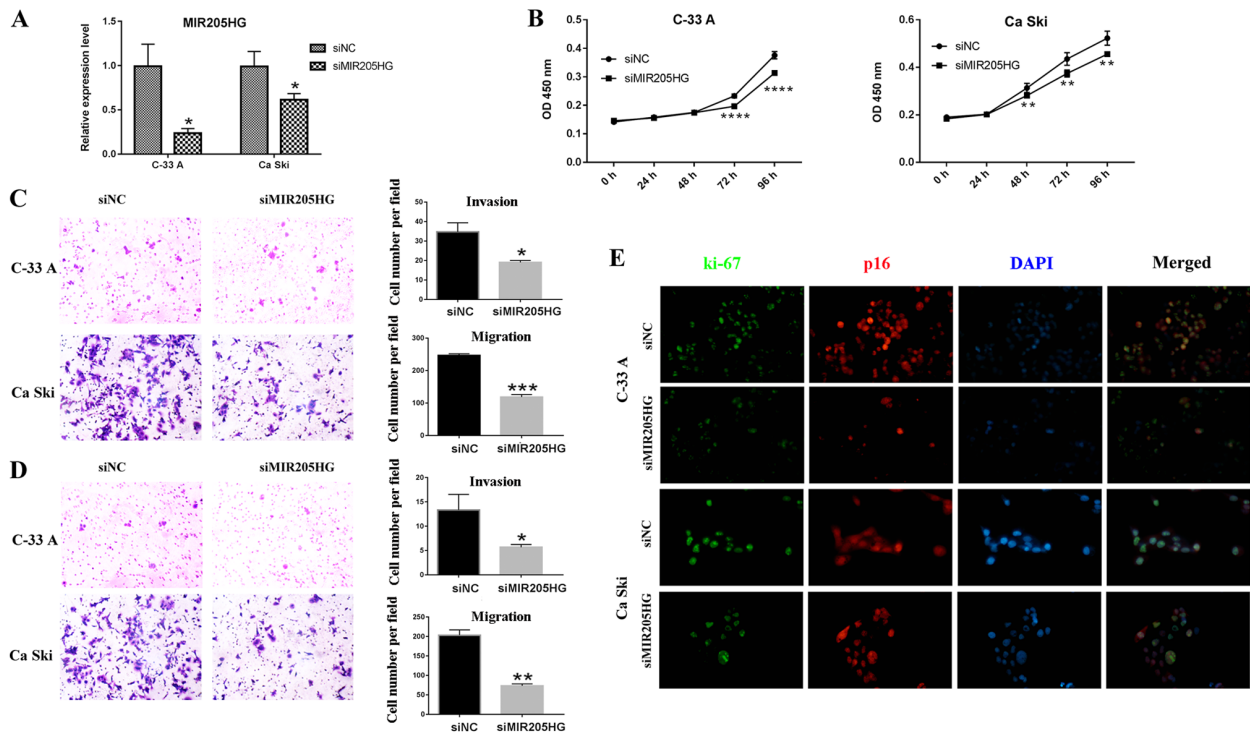


Figure 4. MIR205HG promoted the proliferation and migratory and invasive abilities of CESC cells. (A) MIR205HG knockdown efficiency was detected by reverse transcription quantitative PCR. Two-tailed student's t-test. * $P < 0.05$. (B) Proliferation of CESC cells assessed by CCK-8 assay. MIR205HG knockdown inhibited CESC cell proliferation. siMIR205HG group was compared with siNC group at the indicated time points. Two-tailed student's t-test. (C and D) On MIR205HG knock down, significant suppression of cell migration and invasion ability in C-33 A and Ca Ski. Transwell results are shown (magnification, $\times 200$). Cell number analysis is shown on the right. Two-tailed student's t-test. * $P < 0.05$, ** $P < 0.01$, *** $P < 0.001$ and **** $P < 0.0001$. (E) Immunofluorescence staining results of Ki-67 (green) and p16 (red). Nuclei were stained with DAPI (blue). Magnification, $\times 400$. CESC, cervical squamous cell carcinoma and endocervical adenocarcinoma; NC, negative control; si, small interfering.

MIR205HG knockdown (Fig. 4C and D). The migratory and invasive abilities of Ca Ski cells appeared to be higher than that of C-33 A cells. Immunofluorescence staining of p16 and Ki-67 was then performed (Fig. 4E). Ki-67 staining, which is the marker of proliferation, was decreased in C-33 A following MIR205HG knockdown, and was partially decreased in Ca Ski. In addition, p16 fluorescence intensity was lower in

C-33 A cells after MIR205HG knockdown, whereas no change was observed in Ca Ski cells.

Network analysis of MIR205HG. A network between MIR205HG and its coexpressed genes were analyzed by cytoscape3.6.1 (Fig. 5A). Genes in enriched pathways were selected. A total of 49 related genes are presented. Subsequently, the

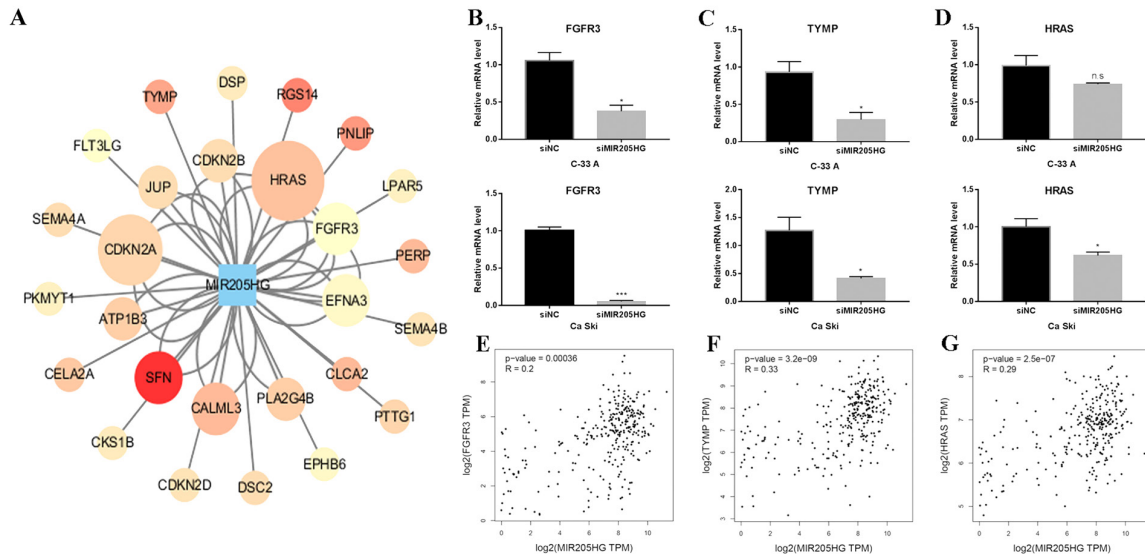


Figure 5. Network analysis of MIR205HG co-expression genes. (A) Network analysis showed the relationship between MIR205HG and co-expressed genes. Red nodes indicate a high correlation. (B) *FGFR3* mRNA level was significantly decreased following MIR205HG knockdown in C-33 A and Ca Ski cells. (C) RT-qPCR showed that the expression of *TYMP* in C-33 A and Ca Ski transfected with siMIR205HG was significantly downregulated. (D) RT-qPCR showed that expression of *HRAS* in Ca Ski cells transfected with siMIR205HG was significantly downregulated, whereas it was not significant in C-33 A. Two-tailed student's t-test in B, C and D. * $P < 0.01$ and *** $P < 0.001$. (E-G) Correlation between MIR205HG and *FGFR3*, *TYMP*, and *HRAS* using TCGA CESC data, respectively. NC, negative control; si, small interfering; ns, non-significant; *FGFR3*, fibroblast growth factor receptor 3; *TYMP*, thymidine phosphorylase; *HRAS*, GTPase HRas; RT-qPCR, reverse transcription quantitative PCR.

expression of three selected genes, *FGFR3*, *TYMP* and *HRAS*, was detected in MIR205HG knocked down CESC cells. In C-33 A cells, all these genes were significantly downregulated after MIR205HG knockdown (Fig. 5B-D), whereas *HRAS* showed no significant change (Fig. 5D). Furthermore, the expression of these three genes was positively correlated with MIR205HG expression in CESC data of TCGA (Fig. 5E-G).

Discussion

Previous studies have revealed various functions of lncRNAs in regulating numerous complex biological processes (8-10). For example, HOTAIR enhances cervical cancer aggressiveness by increasing the expression levels of vascular endothelial growth factor, matrix metalloproteinase 9 and epithelial-mesenchymal transition-associated genes (9). The data from TCGA in the present study provided an insight into the differentially expressed lncRNAs in cancer and normal tissues, which were previously reported as promising therapeutic targets, diagnosis biomarkers or prognosis biomarkers. For instance, Gong *et al* (16) selected several lncRNAs differentially expressed in TCGA and RNA-seq data and analyzed them using survival rate. They identified LINC01537 as having a role in the regulation of energy metabolism via phosphodiesterase 2A in lung cancer.

In the present study, 203 differentially expressed lncRNAs were identified in the CESC data retrieved from the TCGA. The top 15 upregulated and downregulated lncRNAs are listed in Table I. LINC00958, the fourth upregulated lncRNA, was reported to promote tumor progression in various types of cancer, including CESC (17,18). EMX2OS, the most down-regulated lncRNA, has been speculated to be a prognostic biomarker for thyroid cancer (19). The roles of other lncRNAs in cervical cancer remain unclear. Luo *et al* (11) analyzed

the expression pattern of differentially expressed lncRNAs and their role in cervical cancer progression, which provides a novel insight into the diagnosis and treatment of cervical cancer. The lncRNA candidates from the present study were different from what they studied.

MIR205HG was the host gene of microRNA (miR)-205 and has not been thoroughly studied to the best of our knowledge. miR-205 has been reported to be commonly downregulated in tumors, in particular in bladder cancer (20). Di Agostino *et al* (12) reported that MIR205HG can promote tumor progression in head and neck squamous cell carcinoma. The present study demonstrated that MIR205HG was overexpressed in CESC tissues compared with normal tissues and promoted the proliferation and migratory and invasive abilities of CESC cells. These findings suggested that MIR205HG may act as a pro-tumor lncRNA in CESC. As a prognostic marker of cervical cancer, p16 is abnormally overexpressed in HPV-positive or negative cervical cancer types (21). MIR205HG knockdown downregulated the expression of p16 in C-33 A cells, whereas no significant change was observed in Ca Ski cells. C-33 A is an HPV-negative cell line, whereas Ca Ski is an HPV-positive cell line. It was reported that p16 is overexpressed in benign tumor and high-grade malignant tumor (21). These findings suggested that the inhibitory effect of MIR205HG on cervical cancer cells might be dependent of the malignancy; however, further investigation is required.

The present study investigated the potential underlying mechanisms of MIR205HG on the regulation of proliferation and invasive ability of CESC cells. The network analysis of MIR205HG related differentially expressed mRNAs was therefore completed and it was found that MIR205HG was co-expressed with 49 genes, including *FGFR3*, *TYMP* and *HRAS*. A recent study revealed the mechanism of MIR205HG which acts as a ceRNA to promote tumor progression by

Table I. Top 15 upregulated and 15 downregulated long non-coding RNAs in cervical squamous cell carcinoma and endocervical adenocarcinoma.

lncRNA	log ₂ (fold-change)	P-value	Description
MIR205HG	7.508	3.08x10 ⁻⁰⁷	MIR205 host gene (non-protein coding)
FAM83H-AS1	4.328	2.67x10 ⁻¹²	FAM83H antisense RNA 1 (head to head)
LINC00925	3.691	7.19x10 ⁻¹⁰	Long intergenic non-protein coding RNA 925
LINC00958	3.544	3.77x10 ⁻⁰⁸	Long intergenic non-protein coding RNA 958
LINC00511	3.512	6.06x10 ⁻²²	Long intergenic non-protein coding RNA 511
LINC01133	2.673	1.05x10 ⁻³	Long intergenic non-protein coding RNA 1133
MALAT1	2.525	2.39x10 ⁻³	Metastasis associated lung adenocarcinoma transcript 1 (non-protein coding)
APOC4-APOC2	2.365	2.29x10 ⁻⁰⁴	APOC4-APOC2 readthrough (NMD candidate)
CRNDE	2.112	6.53x10 ⁻⁰⁴	Colorectal neoplasia differentially expressed (non-protein coding)
MIR4435-2HG	2.025	2.89x10 ⁻¹¹	MIR4435-2 host gene
TINCR	1.976	7.06x10 ⁻³	Tissue differentiation-inducing non-protein coding RNA
DGUOK-AS1	1.919	9.88x10 ⁻⁰⁷	DGUOK antisense RNA 1
LINC00467	1.833	7.61x10 ⁻⁰⁹	Long intergenic non-protein coding RNA 467
UNC5B-AS1	1.781	6.64x10 ⁻⁰⁴	UNC5B antisense RNA 1
CDKN2B-AS1	1.715	1.35x10 ⁻¹¹	CDKN2B antisense RNA 1
WT1-AS	-3.407	2.11x10 ⁻³²	WT1 antisense RNA
LINC01088	-3.456	4.83x10 ⁻²³	Long intergenic non-protein coding RNA 1088
FRMD6-AS2	-3.516	1.03x10 ⁻⁶¹	FRMD6 antisense RNA 2
SOCS2-AS1	-3.537	2.51x10 ⁻³³	SOCS2 antisense RNA 1
MIR497HG	-3.567	1.63x10 ⁻³⁸	mir-497-195 cluster host gene (non-protein coding)
ZNF667-AS1	-3.601	2.57x10 ⁻⁰⁶	ZNF667 antisense RNA 1 (head to head)
TRHDE-AS1	-3.644	1.65x10 ⁻³²	TRHDE antisense RNA 1
HSPB2-C11orf52	-3.813	2.21x10 ⁻⁵²	HSPB2-C11orf52 readthrough (NMD candidate)
MIR143HG	-4.401	2.07x10 ⁻⁷³	MIR143 host gene (non-protein coding)
MAGI2-AS3	-4.46	7.03x10 ⁻⁴²	MAGI2 antisense RNA 3
PGM5-AS1	-4.569	1.63x10 ⁻⁵⁵	PGM5 antisense RNA 1
EMX2OS	-4.652	6.45x10 ⁻²¹	EMX2 opposite strand/antisense RNA
HAND2-AS1	-4.956	6.91x10 ⁻⁶⁷	HAND2 antisense RNA 1 (head to head)
DIO3OS	-5.252	1.1x10 ⁻²⁴	DIO3 opposite strand/antisense RNA (head to head)
MEG3	-6.572	6.13x10 ⁻³⁰	Maternally expressed 3 (non-protein coding)

sponging miR-122-5p in cervical cancer (22). The results from network analysis provided additional candidates regulated by MIR205HG in the present study. *FGFR3*, *TYMP* and *HRAS* were demonstrated to be positively correlated with MIR205HG. In addition, the expression of these three genes was downregulated following MIR205HG knockdown. *FGFR3* serves an essential role in the regulation of progenitor cell proliferation, differentiation and apoptosis during the development of the embryo (23). It was reported that *FGFR3* is overexpressed or mutated in numerous types of cancer and can act as an oncogene, in particular in bladder cancer (24-26). *HRAS* is a small GTPase belonging to the Ras family of proteins, which has been broadly studied in cancer (27,28). The results from the present study revealed a significant association between MIR205HG and *FGFR3*, *TYMP* and *HRAS* following bioinformatic analysis and experimental results. However, the underlying mechanism of MIR205HG regulating these genes remains to be elucidated.

In conclusion, the present study determined differentially expressed lncRNAs in CESC and reported MIR205HG as being upregulated in CESC tissues compared with normal tissues. MIR205G knockdown decreased the proliferation and migratory and invasive abilities of CESC cells. Furthermore, the expression of MIR205HG was positively correlated with expression of the oncogenes *HRAS*, *FGFR3* and *TYMP*. The findings from this study suggested that MIR205HG may have pro-tumor function in CESC.

Acknowledgements

Not applicable.

Funding

No funding was received.

Availability of data and materials

The datasets used and/or analyzed during the current study are available from the corresponding author on request.

Authors' contributions

YZ and LZ conceived and designed the study. LY, YZ and LZ performed the experiments and analyzed data. LY wrote the paper. YZ and LZ reviewed and edited the manuscript. All authors read and approved the final manuscript.

Ethics approval and consent to participate

Not applicable.

Patient consent for publication

Not applicable.

Competing interests

The authors declare that they have no competing interests.

References

- Bray F, Ferlay J, Soerjomataram I, Siegel RL, Torre LA and Jemal A: Global cancer statistics 2018: GLOBOCAN estimates of incidence and mortality worldwide for 36 cancers in 185 countries. *CA Cancer J Clin* 68: 394-424, 2018.
- Wentzensen N, Clarke MA, Bremer R, Poitras N, Tokugawa D, Goldhoff PE, Castle PE, Schiffman M, Kingery JD, Grewal KK, *et al*: Clinical evaluation of human papillomavirus screening with p16/Ki-67 dual stain triage in a large organized cervical cancer screening program. *JAMA Intern Med* 179: 881-888, 2019.
- Siegel RL, Miller KD and Jemal A: Cancer statistics, 2019. *CA Cancer J Clin* 69: 7-34, 2019.
- Cohen PA, Jhingran A, Oaknin A and Denny L: Cervical cancer. *Lancet* 393: 169-182, 2019.
- Arun G, Diermeier SD and Spector DL: Therapeutic targeting of long non-coding RNAs in cancer. *Trends Mol Med* 24: 257-277, 2018.
- Wang CJ, Zhu CC, Xu J, Wang M, Zhao WY, Liu Q, Zhao G and Zhang ZZ: The lncRNA UCA1 promotes proliferation, migration, immune escape and inhibits apoptosis in gastric cancer by sponging anti-tumor miRNAs. *Mol Cancer* 18: 115, 2019.
- Qin G, Tu X, Li H, Cao P, Chen X, Song J, Han H, Li Y, Guo B, Yang L, *et al*: lncRNA PSTAR promotes p53 signaling by inhibiting hnRNP K deSUMOylation and suppresses hepatocellular carcinoma. *Hepatology* 2019.
- Bartonicek N, Maag JL and Dinger ME: Long noncoding RNAs in cancer: Mechanisms of action and technological advancements. *Mol Cancer* 15: 43, 2016.
- Kim HJ, Lee DW, Yim GW, Nam EJ, Kim S, Kim SW and Kim YT: Long non-coding RNA HOTAIR is associated with human cervical cancer progression. *Int J Oncol* 46: 521-530, 2015.
- Huang L, Liao LM, Liu AW, Wu JB, Cheng XL, Lin JX and Zheng M: Overexpression of long noncoding RNA HOTAIR predicts a poor prognosis in patients with cervical cancer. *Arch Gynecol Obstet* 290: 717-723, 2014.
- Luo W, Wang M, Liu J, Cui X and Wang H: Identification of a six lncRNAs signature as novel diagnostic biomarkers for cervical cancer. *J Cell Physiol* 235: 993-1000, 2019.
- Di Agostino S, Valenti F, Sacconi A, Fontemaggi G, Pallocca M, Pulito C, Ganci F, Muti P, Strano S and Blandino G: Long non-coding MIR205HG depletes Hsa-miR-590-3p leading to unrestrained proliferation in head and neck squamous cell carcinoma. *Theranostics* 8: 1850-1868, 2018.
- Profumo V, Forte B, Percio S, Rotundo F, Doldi V, Ferrari E, Fenderico N, Dugo M, Romagnoli D, Benelli M, *et al*: LEADeR role of miR-205 host gene as long noncoding RNA in prostate basal cell differentiation. *Nat Commun* 10: 307, 2019.
- Percio S, Rotundo F and Gandellini P: Gene expression dataset of prostate cells upon MIR205HG/LEADR modulation. *Data Brief* 29: 105139, 2020.
- Livak KJ and Schmittgen TD: Analysis of relative gene expression data using real-time quantitative PCR and the 2(-Delta Delta C(T)) method. *Methods* 25: 402-408, 2001.
- Gong W, Yang L, Wang Y, Xian J, Qiu F, Liu L, Lin M, Feng Y, Zhou Y and Lu J: Analysis of survival-related lncRNA landscape identifies a role for LINC01537 in energy metabolism and lung cancer progression. *Int J Mol Sci* 20: 3713, 2019.
- Wang Z, Zhu X, Dong P and Cai J: Long noncoding RNA LINC00958 promotes the oral squamous cell carcinoma by sponging miR-185-5p/YWHAZ. *Life Sci* 242: 116782, 2019.
- Zhao H, Zheng GH, Li GC, Xin L, Wang YS, Chen Y and Zheng XM: Long noncoding RNA LINC00958 regulates cell sensitivity to radiotherapy through RRM2 by binding to microRNA-5095 in cervical cancer. *J Cell Physiol* 234: 23349-23359, 2019.
- Gu Y, Feng C, Liu T, Zhang B and Yang L: The downregulation of lncRNA EMX2OS might independently predict shorter recurrence-free survival of classical papillary thyroid cancer. *PLoS One* 13: e0209338, 2018.
- Gulia C, Baldassarra S, Signore F, Rigon G, Pizzuti V, Gaffi M, Briganti V, Porrello A and Piergentili R: Role of non-coding RNAs in the etiology of bladder cancer. *Genes (Basel)* 8: 339, 2017.
- Romagosa C, Simonetti S, López-Vicente L, Mazo A, Leonart ME, Castellvi J and Cajal SR: p16(Ink4a) overexpression in cancer: A tumor suppressor gene associated with senescence and high-grade tumors. *Oncogene* 30: 2087-2097, 2011.
- Li Y, Wang H and Huang H: Long non-coding RNA MIR205HG function as a ceRNA to accelerate tumor growth and progression via sponging miR-122-5p in cervical cancer. *Biochem Biophys Res Commun* 514: 78-85, 2019.
- Inglis-Broadgate SL, Thomson RE, Pellicano F, Tartaglia MA, Pontikis CC, Cooper JD and Iwata T: FGFR3 regulates brain size by controlling progenitor cell proliferation and apoptosis during embryonic development. *Dev Biol* 279: 73-85, 2005.
- Kandimalla R, Masius R, Beukers W, Bangma CH, Orntoft TF, Dyrskjot L, van Leeuwen N, Lingsma H, van Tilborg AAG and Zwarthoff EC: A 3-plex methylation assay combined with the FGFR3 mutation assay sensitively detects recurrent bladder cancer in voided urine. *Clin Cancer Res* 19: 4760-4769, 2013.
- Javidi-Sharifi N, Traer E, Martinez J, Gupta A, Taguchi T, Dunlap J, Heinrich MC, Corless CL, Rubin BP, Druker BJ and Tyner JW: Crosstalk between KIT and FGFR3 promotes gastrointestinal stromal tumor cell growth and drug resistance. *Cancer Res* 75: 880-891, 2015.
- Pouessel D, Neuzillet Y, Mertens LS, van der Heijden MS, de Jong J, Sanders J, Peters D, Leroy K, Manceau A, Maille P, *et al*: Tumor heterogeneity of fibroblast growth factor receptor 3 (FGFR3) mutations in invasive bladder cancer: Implications for perioperative anti-FGFR3 treatment. *Ann Oncol* 27: 1311-1316, 2016.
- He F, Melamed J, Tang MS, Huang C and Wu XR: Oncogenic HRAS activates epithelial-to-mesenchymal transition and confers stemness to p53-deficient urothelial cells to drive muscle invasion of basal subtype carcinomas. *Cancer Res* 75: 2017-2028, 2015.
- Murugan AK, Grieco M and Tsuchida N: RAS mutations in human cancers: Roles in precision medicine. *Semin Cancer Biol* 59: 23-35, 2019.